

Research Paper

Creep Behavior of Cylinders Subjected to an Internal Pressure and a Two Dimensional Temperature Field Using First Order Shear Deformation Theory

H. Seddighi¹, M. Ghannad^{1,*}, A. Loghman²

¹*Department of Solid Mechanics, Faculty of Mechanical Engineering, Shahrood University of Technology, Shahrood, Iran*

²*Department of Solid Mechanics, Faculty of Mechanical Engineering, University of Kashan, Kashan, Iran*

Received 15 June 2023; accepted 13 August 2023

ABSTRACT

In this paper, the creep analysis in a thick-walled cylinder subjected to internal pressure and heat flux at the inner and outer surfaces has been investigated. The displacement field is obtained based on the first-order shear deformation theory and the thermal field is assumed two-dimensional through the thickness and along cylinder whose in radial direction the thermal field is considered linear. The equilibrium equations of the mechanical and thermal fields were derived using the energy method and the principle of virtual work for mechanical loading and heat flux. The creep behavior is described by Bailey-Norton's time-dependent creep law. Analytical solutions with iteration methods have been used to obtain the stresses, strains, and displacement. The relationship between the temperature and the creep deformation was investigated by examining changes in the radial displacement by increasing the temperature by two to three times at a specific point. The effects of parameters such as pressure, heat flux and radial displacement at different temperatures on stress distribution were discussed. It was shown the circumferential stress accounts for the most changes caused by creep behavior. The presented method provides a semi-analytical solution to investigate the creep behavior of the thick-walled cylinders, which can be used for purposes such as designing and their optimization and parametric study under real temperature loading conditions.

© 2023 IAU, Arak Branch. All rights reserved.

Keywords : Cylinder; Stress; Heat flux; Pressure; Displacement.

1 INTRODUCTION

GIVEN the structures and equipment function under long-term mechanical and thermal loads, the creep phenomenon is inevitable. Therefore, the investigation of a more accurate analysis of structures and a better assessment of their life period is essential [1-3]. Cylindrical and spherical shells have vast applications in pressure

*Corresponding author.

E-mail address: ghannad.mehdi@gmail.com (M. Ghannad)

vessels. Therefore, creep studies for these structures in various loading conditions, including mechanical, thermal, and magnetic loads, have been performed [4,5]. The first studies about the creep phenomenon started in the 60s. Jones and Sullivan [6] investigated the creep buckling of a long cylindrical shell. In the same period, Stowell [7] studied the biaxial creep of aluminum alloy tubes under thermal loading. Johnson also described the creep behavior of metallic thick-walled cylinders under internal and external pressure and torque and thermal gradient. King [8] presented an experimental and theoretical study of the creep deformation of a thick-walled cylinder under internal pressure. Gupta et al. [9] determined the stresses of a circular cylinder of compressible material subjected to torsion they showed the shear stress for a compressible material is greater than incompressible material. Murakami [10] investigated the effect of shell geometry and the non-linearity of the creep law on simply-supported cylindrical shells. Bhatnagar [11] was one of the first researchers who investigated the creep behavior of anisotropic materials. He studied the secondary creep of cylindrical shells in plane strain conditions in different orthotropic materials. Loghman and Wahab [12] evaluate the creep damage of thick-walled tubes using the projection concept. Subsequently, creep studies took on a specific form and classification. Several studies assume the stress level and creep rate structures to be constant and not change with time. You et al. [13] examined how a variation of material properties in radial direction affects stress in functionally graded vessels. Altenbach et al. [14] examined the steady state creep of a thick pressurized cylinder with two distinct creep behaviors, linear and power law. (ii) The second investigation is about the time-dependent creep behavior of cylindrical shells that obtained the histories of stresses and creep rates during steady-state creep. Loghman and Atabakhshian [15] performed research on the time-dependent creep of a rotating cylinder made of anisotropic exponentially graded material (EGM). Thakur [16] investigated the effect of anisotropic material on creep behavior of thick-walled cylinder under combined axial load and internal pressure. They found the anisotropy of the material has little effect on radial stress but the effect is more prominent on the axial and tangential stresses for higher anisotropic constant along the radius. Moradi and Loghman [17] advanced this research to analyze time-dependent creep under a non-axisymmetric thermal field and internal pressure for a thick-walled cylinder. The effect of particle content, size, and temperature on the magneto-thermo-mechanical creep behavior of composite cylinders were investigated by Loghman et al. [18]. Wahab and Ahmad [19] considered internal heat generation in a functionally graded rotating cylinder vessel and presented thermoelastic and creep analysis. In another research Thakur et al. [20] by using Seth's theory studied creep strain rates in the circular cylinder under temperature gradient materials by finite deformation. They showed the maximum value of strain rates occurs at the external surface of an incompressible material as compared to the compressible materials. In the mentioned papers, creep studies were in particular conditions, meaning plane strain and plane stress. In more general conditions, such as different boundary conditions, thermoelastic analysis with shear deformation theory and semi-analytical solution in creep studies could be used. The time-dependent thermomechanical creep behavior of an FGM thick-hollow cylinder shell under non-uniform internal pressure was determined by Kashkoui and Tahan [21]. The thermal field was assumed uniform from the inner to the outer surface. Mechanical and thermal properties, except the Poisson's ratio, were considered a power function along the thickness, and the constitutive creep model is based on Norton's Law. Stress and displacement distribution have been obtained for a relatively long time using the FSDT theory for thermoelastic analysis and an iterative method for creep analysis. In the following, Kashkoui et al. [22] investigated the creep of an FGM cylindrical vessel with variable thickness using a multi-layer method (MLM) method. It was shown that the temperature gradient has a significant influence on the creep response of the pressure vessel. The studies by this researcher extended previous works on structure life during creep [23], in which, creep damage has been considered based on the FSDT theory and the Larson-Miller parameter. Ghannad and Parhizkar Yaghoobi [24] studied the temperature distribution in cylindrical shells. They clarified that temperature could vary in both longitudinal and radial directions. Therefore, the first-order shear deformation theory (FSDT) has been completed into the first-order temperature theory (FTT). Using FSDT, they [25] applied the mentioned theory to an FG cylinder under thermomechanical loads using the first-order temperature theory. They showed that the shear stress value is significant at the boundaries, and temperature, displacement field and stresses are strongly dependent on the length.

The aim of this research is to analyze the creep of the cylinder by considering the actual conditions of temperature and pressure axisymmetric loading. In such a way that by using the theory of shear deformation, the effect of shear stress can be seen in the boundaries of the cylinder and the temperature field distribution can be considered in two dimensions of the cylinder. Unlike the common simplification that usually considers the temperature distribution only along the cylinder thickness. This method is capable of creep analysis for thick-walled cylinders under axially symmetric thermal and mechanical loadings and you can use this method to design, parametric study and optimization of the cylinders.

2 ANALYSIS

Consider a thick-walled cylindrical shell with inner radius r_i , outer radius r_o and, respectively, length L , Young's modulus E , and Poisson's ratio ν , are considered. The heat flux from the inner and outer surface to the surrounding ambient are considered (Fig. 1).

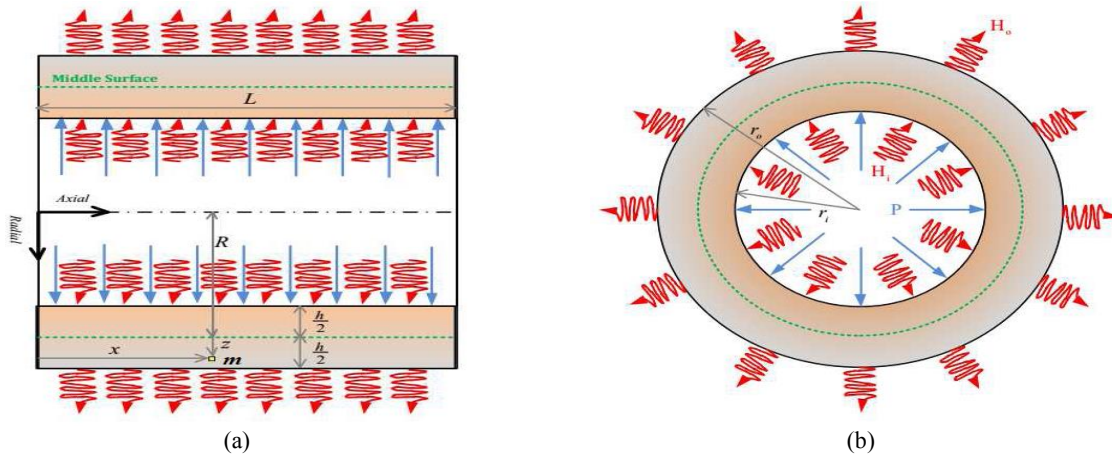


Fig.1
The cross-section of the thick cylinder under pressure and heat flux.

The location of the typical point 'm' is function of (r,x) that based on the shear deformation theory can be written the function of $(R+z, x)$

$$m; (r, x) = (R + z, x) \quad (1)$$

where R is the distance of the middle surface from the axial direction, and z is the distance of the specific point from the middle surface.

Specifically, z and x are in the range of $-h/2 \leq z \leq h/2, 0 \leq x \leq L$, where h is the thickness of the cylinder. Temperature changes from the reference temperature $(\theta = T - T^*)$ and displacement field (U_z, U_x) and the temperature field are described as follows [24];

$$\begin{cases} U_x(x, z) = u(x) + \phi(x)z \\ U_\theta(x, z) = 0 \\ U_z(x, z) = w(x) + \psi(x)z \\ \theta(x, z) = \theta(x) + \Gamma(x)z \end{cases} \quad (2)$$

where, $u(x), w(x)$ are the displacement component and $\theta(x)$ is the thermal component. $\phi(x), \psi(x), \Gamma(x)$ are the functions expressing displacement and temperature variation fields. The kinematic equations given by [24];

$$\begin{cases} \varepsilon_x = \frac{\partial U_x}{\partial x} = \frac{du}{dx} + z \frac{d\phi}{dx} \\ \varepsilon_\theta = \frac{U_z}{r} = \frac{w + \psi z}{R + z} = \frac{w}{R + z} + \frac{\psi}{R + z} z \\ \varepsilon_z = \frac{\partial U_z}{\partial z} = \psi \\ \gamma_{xz} = \frac{\partial U_x}{\partial z} + \frac{\partial U_z}{\partial x} = \phi(x) + \frac{dw}{dx} + \frac{d\psi}{dx} z \end{cases} \quad (3)$$

The thermal field-temperature variation is defined as [24]:

$$\begin{aligned}
 e_z &= -\frac{\partial \theta}{\partial z} = -\Gamma(x) \\
 e_x &= -\frac{\partial \theta}{\partial x} = -\frac{d\theta}{dx} - \frac{d\Gamma}{dx} z
 \end{aligned}
 \tag{4}$$

The constitutive equations for isotropic materials, considering the creep phenomenon, are as follows [26]:

$$\begin{cases}
 \begin{Bmatrix} \sigma_x \\ \sigma_\theta \\ \sigma_z \end{Bmatrix} = \frac{E}{(1+\nu)(1-2\nu)} \begin{bmatrix} (1-\nu) & \nu & \nu \\ \nu & (1-\nu) & \nu \\ \nu & \nu & (1-\nu) \end{bmatrix} \begin{Bmatrix} \varepsilon_x - \varepsilon_x^C \\ \varepsilon_\theta - \varepsilon_\theta^C \\ \varepsilon_z - \varepsilon_z^C \end{Bmatrix} - \frac{E}{(1-2\nu)} \alpha \theta \\
 \tau_{xz} = \frac{E}{2(1+\nu)} \{ \gamma_{xz} - 2\varepsilon_{xz}^C \} \\
 \begin{Bmatrix} h_z \\ h_x \end{Bmatrix} = \begin{bmatrix} \kappa & 0 \\ 0 & \kappa \end{bmatrix} \begin{Bmatrix} e_z \\ e_x \end{Bmatrix}
 \end{cases}
 \tag{5}$$

where, ε_i , h_i , ε_i^C and e_i are respectively the stresses, strains, heat fluxes, creep strains and thermal field in the axial, circumferential and radial directions (x, θ, z) . E, ν, k, α are, respectively modulus of elasticity, Poisson's ratio, thermal expansion coefficient, and thermal conduction coefficient.

The thermal and mechanical resultant is defined as:

$$\begin{cases}
 \begin{Bmatrix} N_x^m \\ N_\theta^m \\ N_z^m \end{Bmatrix} = \int_{-\frac{h}{2}}^{\frac{h}{2}} \begin{Bmatrix} \sigma_x(1+z/R) \\ \sigma_\theta \\ \sigma_z(1+z/R) \end{Bmatrix} dz \\
 \begin{Bmatrix} M_x^m \\ M_\theta^m \\ M_z^m \end{Bmatrix} = \int_{-\frac{h}{2}}^{\frac{h}{2}} \begin{Bmatrix} \sigma_x(1+z/R) \\ \sigma_\theta \\ \sigma_z(1+z/R) \end{Bmatrix} z dz
 \end{cases}
 \tag{6}$$

$$\begin{cases}
 \begin{Bmatrix} Q_x^m \\ M_{xz}^m \end{Bmatrix} = \int_{-\frac{h}{2}}^{\frac{h}{2}} \begin{Bmatrix} \tau_{xz}(1+z/R) \\ \tau_{xz}z(1+z/R) \end{Bmatrix} dz \\
 \begin{Bmatrix} N_x^t \\ N_z^t \end{Bmatrix} = \int_{-\frac{h}{2}}^{\frac{h}{2}} \begin{Bmatrix} h_x(1+z/R) \\ h_z(1+z/R) \end{Bmatrix} dz \\
 M_x^t = \int_{-\frac{h}{2}}^{\frac{h}{2}} h_x(1+z/R) z dz
 \end{cases}
 \tag{7}$$

Based on virtual work, the variations of thermo-mechanical energy are equal to the external thermo-mechanical work.

$$\delta U = \delta W \quad (8)$$

The thermo-mechanical energy and the external work are [27]:

$$U = \int U^* dv, dv = rd\theta dx dz = (R+z) dx d\theta dz$$

$$U^* = \frac{1}{2}(\sigma_x \varepsilon_x + \sigma_\theta \varepsilon_\theta + \sigma_z \varepsilon_z + \tau_{xz} \gamma_{xz} - h_z e_z - h_x e_x) \quad (9)$$

$$W = \iint \left((P_{iz} U_z |_{r=ri} - H_i \delta\theta |_{r=ri}) - (P_{oz} \delta U_z |_{r=ro} - H_o \delta\theta |_{r=ro}) \right) ds,$$

$$ds = rd\theta dx$$

Their variation is as follow is given by [24]:

$$\delta U = \int_0^L \int_0^{2\pi} \int_{-\frac{h}{2}}^{\frac{h}{2}} (\sigma_z \delta\varepsilon_z + \sigma_x \delta\varepsilon_x + \sigma_\theta \delta\varepsilon_\theta + \tau_{xz} \delta\gamma_{xz} - h_z \delta e_z - h_x \delta e_x) (R+z) dz d\theta dx \quad (10)$$

$$\delta W = \int_0^L \int_0^{2\pi} \left((P_{iz} \delta U_z |_{r=ri} - H_i \delta\theta |_{r=ri}) \left(R - \frac{h}{2} \right) - (P_{oz} \delta U_z |_{r=ro} - H_o \delta\theta |_{r=ro}) \left(R + \frac{h}{2} \right) \right) d\theta dx$$

Substituting Eqs. (9) -(10) into Eqs. (11), we gets:

$$\begin{cases} R \frac{dN_x^m}{dx} = 0 \\ R \frac{dM_x^m}{dx} - RQ_x^m = 0 \\ R \frac{dQ_x^m}{dx} - N_\theta^m = -P_{zi} \left(R - \frac{h}{2} \right) + P_{zo} \left(R + \frac{h}{2} \right) \\ R \frac{dM_{xz}^m}{dx} - M_\theta^m - RN_z^m = P_{zi} \frac{h}{2} \left(R - \frac{h}{2} \right) + P_{zo} \frac{h}{2} \left(R + \frac{h}{2} \right) \\ R \frac{dN_x^t}{dx} = H_i \left(R - \frac{h}{2} \right) - H_o \left(R + \frac{h}{2} \right) \\ R \frac{dM_x^t}{dx} - RN_z^t = -H_i \frac{h}{2} \left(R - \frac{h}{2} \right) - H_o \frac{h}{2} \left(R + \frac{h}{2} \right) \end{cases} \quad (11)$$

Boundary conditions at the two ends of the cylinder is given by [24]:

$$\left[N_x^m \delta u + M_x^m \delta\phi + Q_x^m \delta w + M_{xz}^m \delta\psi + N_x^t \delta\theta + M_x^t \delta\Gamma \right] |_{0 \& L} = 0 \quad (12)$$

Substituting Eqs. (11) -(12) into Eq. (13), the set of differential Eq. (13) is as follows:

$$[A] \frac{d^2}{dx^2} \{y\} + [B] \frac{d}{dx} \{y\} + [C] \{y\} = \{f\} \quad (13)$$

$$\{y\} = \{u \quad \phi \quad w \quad \psi \quad \theta \quad \Gamma\}^T$$

$[A]_{6 \times 6}, [B]_{6 \times 6}, [C]_{6 \times 6}$ are the coefficient matrixes and $\{f\}$ is the force vector.

3 THERMOELASTIC ANALYSIS

The creep strains must be ignored before a thermoelastic solution may be obtained. To solve the set of differential Eq (14), $\{y\}$ is changed to $\{y^*\}$, and the first and fifth equations are integrated.

$$\begin{aligned}
 [A^*] \frac{d^2}{dx^2} \{y^*\} + [B^*] \frac{d}{dx} \{y^*\} + [C^*] \{y^*\} &= \{f\} \\
 \{y^*\} &= \left\{ \frac{du}{dx} \quad \phi \quad w \quad \psi \quad \theta \quad \Gamma \right\}^T
 \end{aligned}
 \tag{14}$$

where:

$$\begin{aligned}
 [A^*] &= \begin{bmatrix} 0 & 0 & 0 & 0 & 0 & 0 \\ 0 & (1-\nu)R h^3/12 & 0 & 0 & 0 & 0 \\ 0 & 0 & \mu R h & \mu h^3/12 & 0 & 0 \\ 0 & 0 & \mu h^3/12 & \mu R h^3/12 & 0 & 0 \\ 0 & 0 & 0 & 0 & 0 & 0 \\ 0 & 0 & 0 & 0 & -\kappa h^3/12 & -\kappa R h^3/12 \end{bmatrix} \\
 [B^*] &= \begin{bmatrix} 0 & (1-\nu)h^3/12 & \nu h & \nu R h & -(1+\nu)\alpha R h & -(1+\nu)\alpha h^3/12 \\ (1-\nu)h^3/12 & 0 & -\mu R h & -(\mu-2\nu)h^3/12 & -(1+\nu)\alpha h^3/12 & -(1+\nu)\alpha R h^3/12 \\ 0 & \mu R h & 0 & 0 & 0 & 0 \\ 0 & (\mu-2\nu)h^3/12 & 0 & 0 & 0 & 0 \\ 0 & 0 & 0 & 0 & 0 & 0 \\ 0 & 0 & 0 & 0 & 0 & 0 \end{bmatrix} \\
 [C^*] &= \begin{bmatrix} R h(1-\nu) & 0 & \nu h & \nu R h & -(1+\nu)\alpha R h & -(1+\nu)\alpha h^3/12 \\ 0 & -\mu R h & 0 & 0 & 0 & 0 \\ -\nu h & 0 & -(1+\nu)\beta & -(h-(1-\nu)R\beta) & (1+\nu)\alpha h & 0 \\ -\nu R h & 0 & (h-(1-\nu)R\beta) & -(1+\nu)R^2\beta & R(1+\nu)\alpha h & 2(1+\nu)\alpha h^3/12 \\ 0 & 0 & 0 & 0 & -\kappa R h & -\kappa h^3/12 \\ 0 & 0 & 0 & 0 & 0 & -\kappa R h \end{bmatrix} \\
 \{f^*\} &= \left\{ \begin{array}{l} \frac{C_0}{R} \\ 0 \\ -\frac{R}{\lambda E} \left[P_{zi} \left(1 - \frac{h}{2R} \right) - P_{zo} \left(1 + \frac{h}{2R} \right) \right] \\ \frac{R h}{2 \lambda E} \left[P_{zi} \left(1 - \frac{h}{2R} \right) + P_{zo} \left(1 + \frac{h}{2R} \right) \right] + \\ (H_i (R - \frac{h}{2}) - H_o (R + \frac{h}{2})) \frac{x^2}{2} + C_9 x + C_{10} \\ -H_i \frac{h}{2} (R - \frac{h}{2}) - H_o \frac{h}{2} (R + \frac{h}{2}) \end{array} \right\}
 \end{aligned}$$

And in above equations, the parameters, λ, β, μ are defined as; $\lambda = \frac{1}{(1+\nu)(1-2\nu)}$, $\beta = \ln\left(\frac{R+h/2}{R-h/2}\right)$, $\mu = K_s \frac{(1-2\nu)}{2}$ which K_s (shear correction factor) is considered for cylindrical shell $\frac{5}{6}$. C_0, C_9 , and C_{10} , as the result of integrating, are constant. The solution of the differential Eq. (14) as follows:

$$\{y^*\} = \{y^*\}_g + \{y^*\}_p \quad (15)$$

where $\{y^*\}_g, \{y^*\}_p$ are general and particular solutions, respectively. The general solution is the form of $\{y^*\} = \{\xi\} e^{mix}$ which is obtained from Eq. (15)

$$([A^*]m^2 + [B^*]m + [C^*])\{\xi\}e^{mix} = \{0\} \quad (16)$$

Eq. (16) is the eigenvalue problem for non-trivial solution $e^{mix} \neq 0$ and the coefficient of the determinant must be considered zero.

$$\det([A^*]m^2 + [B^*]m + [C^*]) = 0 \quad (17)$$

The determinant is an eight-order polynomial including four pairs of conjugated roots. By calculating eigenvectors $\{\xi\}_i$ corresponding to eigenvalues, the format of the general solution is;

$$\{y^*\}_g = \sum_{i=1}^8 C_i \{\xi\} e^{mix} \quad (18)$$

The constants C_i are determined by applying boundary conditions. $\{f^*\}$ is a quadratic polynomial. therefore, the particular solution is as follows;

$$\{y^*\}_p = \{y^*\}_{p2} x^2 + \{y^*\}_{p1} x + \{y^*\}_{p0} \quad (19)$$

where $\{y^*\}_{p2}, \{y^*\}_{p1}, \{y^*\}_{p0}$ are unknown coefficients vector, which are obtained by substituting a particular solution in Eq. (18). Therefore, the general solution is;

$$\{y^*\}_g = \sum_{i=1}^8 C_i \{\xi\} e^{mix} + \{y^*\}_{p2} x^2 + \{y^*\}_{p1} x + \{y^*\}_{p0} \quad (20)$$

There are 11 contradictions plus one another, C_{11} which appear in the integration $\{y^*\}$. The 12 constants are determined by applying boundary conditions at the two ends of the cylinder. Boundary conditions could be defined as the displacement and temperature field or displacement and thermal resultants or their combination. Both ends of the cylinder are considered to have $T=50^0 C$ and to be mechanically clamped.

$$x = 0 \& L; \{y\} = \begin{Bmatrix} u \\ \phi \\ \psi \\ \theta \\ \Gamma \end{Bmatrix} = \begin{Bmatrix} 0 \\ 0 \\ 0 \\ 0 \\ T - T^* \\ 0 \end{Bmatrix} \quad (21)$$

The set of differential equations is solved by the software Maple 15. Thus the thermoelastic stresses, strains, and displacements are obtained. Now the creep process can begin.

4 MODELING OF CREEP BEHAVIOR

The Bailey–Norton’s creep constitutive model for the effective strain, is [15]

$$\varepsilon_e = D\sigma_e^N t^m \tag{22}$$

Creep strain rates are related to the stresses and the material uniaxial creep constitutive model by the well-known Prandtl-Reuss equations as follows:

$$\begin{aligned} \dot{\varepsilon}_x^C &= D\sigma_e^{N-1} \left(\sigma_x - \frac{1}{2}(\sigma_\theta + \sigma_z) \right) m t^{m-1}, \\ \dot{\varepsilon}_\theta^C &= D\sigma_e^{N-1} \left(\sigma_\theta - \frac{1}{2}(\sigma_x + \sigma_z) \right) m t^{m-1}, \\ \dot{\varepsilon}_z^C &= D\sigma_e^{N-1} \left(\sigma_z - \frac{1}{2}(\sigma_x + \sigma_\theta) \right) m t^{m-1}, \\ \dot{\varepsilon}_{xz}^C &= \frac{3}{2} D\sigma_{eff}^{N-1} \tau_{xz} m t^{m-1} \end{aligned} \tag{23}$$

where D and N are creep parameters and m is a constant coefficient $1/3 < m < 1/2$. Here the effective stress based on the von Mises criterion is written as:

$$\sigma_e = \frac{1}{\sqrt{2}} \left[\left((\sigma_x - \sigma_\theta)^2 + (\sigma_\theta - \sigma_z)^2 + (\sigma_x - \sigma_z)^2 + 6\tau_{xz}^2 \right) \right]^{1/2} \tag{24}$$

5 TIME- DEPENDENT CREEP ANALYSIS

A semi-analytical method has been used to obtain a history of stresses, strains, and deformations. The creep strains in Eq. (6) must be considered. Based on the iterative method, the set of the differential equations must be considered in the time domain as follows:

$$\begin{aligned} [A^*] \frac{d^2}{dx^2} \{y^*\} + [B^*] \frac{d}{dx} \{y^*\} + [C^*] \{y^*\} &= \{f^*\} \\ \{y^*\} &= \left\{ \frac{du}{dx} \quad \phi \quad w \quad \psi \quad \theta \quad \Gamma \right\}^T \end{aligned} \tag{25}$$

The force vector derivative with respect to time, with internal pressure and heat flux being steady state, is as follows:

$$\{\dot{f}\} = \left\{ \begin{aligned} &\frac{\dot{C}_0}{R} + Rh \left\{ (1-\nu) \frac{h^3}{12} \dot{\varepsilon}_x^C + \nu \frac{h^3}{12} (\dot{\varepsilon}_\theta^C + \dot{\varepsilon}_z^C) \right\} \\ &\frac{h^3}{12} \left\{ (1-\nu) \frac{d\dot{\varepsilon}_x^C}{dx} + \nu \left(\frac{d\dot{\varepsilon}_\theta^C}{dx} + \frac{d\dot{\varepsilon}_z^C}{dx} \right) \right\} - 2\mu h \dot{\varepsilon}_{xz}^C \\ &2\mu Rh \frac{d\dot{\varepsilon}_{xz}^C}{dx} + \left[(1-\nu) h \dot{\varepsilon}_\theta^C + \nu h (\dot{\varepsilon}_x^C + \dot{\varepsilon}_z^C) \right] \\ &2\mu \frac{h^3}{12} \frac{d\dot{\varepsilon}_{xz}^C}{dx} - Rh \left[(1-\nu) \dot{\varepsilon}_z^C + \nu (\dot{\varepsilon}_x^C + \dot{\varepsilon}_\theta^C) \right] \\ &\dot{C}_9 x + \dot{C}_{10} \\ &0 \end{aligned} \right\} \tag{26}$$

And the boundary condition:

$$x = 0 \& L; \{y\} = \begin{Bmatrix} \dot{u} \\ \dot{\phi} \\ \dot{\psi} \\ \dot{\theta} \\ \dot{\Gamma} \end{Bmatrix} = \begin{Bmatrix} 0 \\ 0 \\ 0 \\ 0 \\ 0 \end{Bmatrix} \quad (27)$$

The solution of the set of differential Eq. (24) are:

$$\{y^*\} = \{y^*\}_g + \{y^*\}_p \quad (28)$$

The general solution is the same as the general solution in the thermoelastic analysis

$$\{y^*\}_g = \sum_{i=1}^8 \dot{C}_i \{\xi\} e^{mix} \quad (29)$$

And the form of the particular solution is as follows:

$$\{y^*\}_p = \{y^*\}_{p1} x + \{y^*\}_{p0} \quad (30)$$

By applying boundary condition, $\dot{C}_1 \dots \dot{C}_{12}$ obtained. The iterative method based on the Euler method obtained stresses strains and displacements distribution [27]. In this method, the value of y_{i+1} were determined by linear extrapolation from y_i . Based on the Taylor expansion, we have the following:

$$y_{i+1} = y_i + \Delta t_{i+1} \dot{y}_{i+1} \quad (31)$$

It can be seen that this method is convergent, and the shorter the time interval, the closer the approximate solution will be to the exact solution. Thus y_{i+1} can be $\sigma_i, \varepsilon_i, u_i$ and the histories of stresses, strains, and displacements have been obtained.

Steps of the iterative method:

The cylinder is divided into longitudinal and axial directions:

- 1- The thermoelastic stresses and displacements are considered initial values for the creep process.
- 2- Effective stress is obtained based on the von-Mises criterion.
- 3- An appropriate time increment needs to be picked for timing steps. The total time is the sum of time increments as the creep process advances over time.

$$t_k = \sum_{i=0}^k \Delta t^{(i)} \quad (32)$$

- 4- The creep strain rate increments are obtained from Prandtl-Ruess equations, and their derivatives relatives to x are determined from the definition of derivative by a backward method. These are added to accumulated creep strain rates and their derivative at all divisions all over the cylinder.
- 5- Then, the particular solution $\{y^*\}_p \{\dot{C}_i\}$ is obtained.
- 6- By applying the Euler method, the new increments of stresses, strains, and displacement are determined.

$$\sigma_{ij}^k(z, x, t_k) = \sigma_{ij}^{(k-1)}(z, x, t_k) + \dot{\sigma}_{ij}^k(z, x, t_k) \Delta t_{i+1} \quad (33)$$

- 7- By substituting new values of stresses of the sixth step in the second step, the process will be repeated until convergence is accomplished.

6 RESULT AND DISCUSSION

The cylinder is considered with inner radius $r_i=0.04m$, outer radius $r_o=0.06m$, and length $L=0.8m$. The Young's modulus of elasticity, thermal expansion coefficient, and thermal conduction coefficient of the cylinder are $E = 201Gpa, \alpha = 15.27 \times 10^{-6} / ^\circ C, k=12.15 w/(m^0C)$ [21], the Poisson's ratio is 0.31. The cylinder is subjected to internal pressure $P=80 MPa$, and external heat flux $H_i=300(w/m^2)$ on the inner surface, and heat flux $H_o=180(w/m^2)$ from the outer surface to the surrounding ambient. The reference temperature is assumed to be $T^*=25^\circ C$. The non-dimensional parameters are defined as follows: The Bailey–Norton's creep constitutive constants are $D = 5.2 \times 10^{-56} Mpa^{-N} hr^{-m}, m = 1, N = 5.4$ [21]. Non-dimensional parameters were introduced;

$$r^* = r/r_i, z^* = z/h/2, \sigma_i^* = \sigma/P_i, \sigma_e^* = \sigma_i/P_i, \tau_{xz}^* = \tau_{xz}/P_i, T^* = T/T_0, u^* = u/r_i * 10^3 \tag{34}$$

Figs. 2-8 show the history of stress and displacements after two years. During two years, increasing in stresses is observed, which the most increase related to circumferential stress. Variation in the radial stress occurs very smoothly. Shear stress changes are affected by boundary and loading conditions and the creep phenomenon has no significant effect.

In the middle point, circumferential stress increased. In the first 5,000 hours, it was 6.98%; in the second 5,000 hours, 30.44%; in the third 5,000, 84%, and after two years, 141% compared to the initial time. Fig. 7 indicates radial displacement distribution over time. The initial value increased by 120% after two years. Axial displacement is mainly due to boundary conditions. Due to the symmetry in the cylinder, as shown above in the study, and our intention to see the displacement history at all times, it is seen as a straight line, so it is drawn in two diagrams.

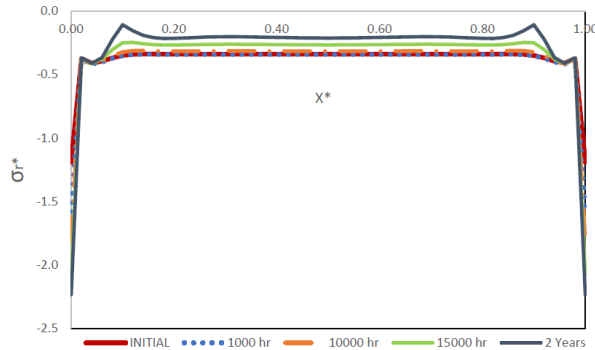


Fig.2 Distribution of normalized radial stress along the dimensionless axial direction after two years of creeping.

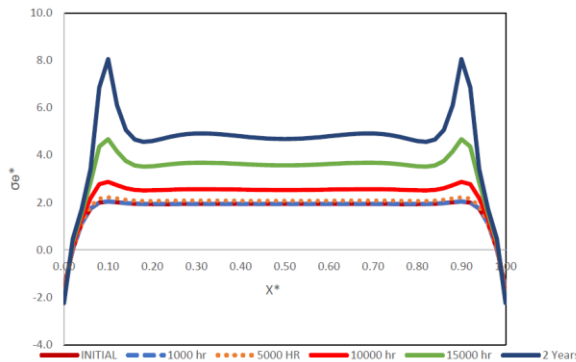


Fig.3 Distribution of normalized circumferential stress along the dimensionless axial direction after two years of creeping.

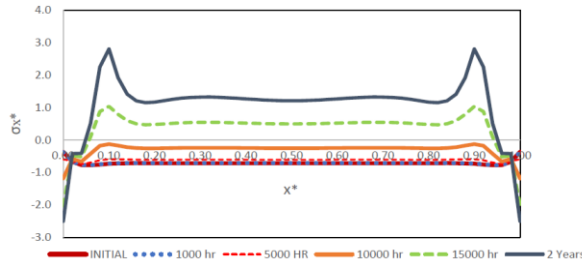


Fig.4
Distribution of normalized axial stress along the dimensionless axial direction after two years of creeping.

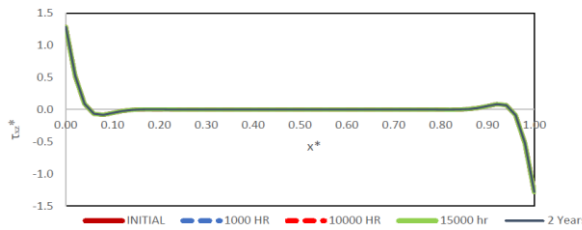


Fig.5
Distribution of normalized shear stress along the dimensionless axial direction after two years of creeping.

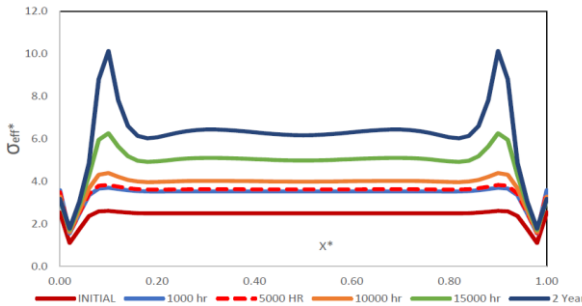


Fig.6
Distribution of effective stress along the dimensionless axial direction after two years of creeping.

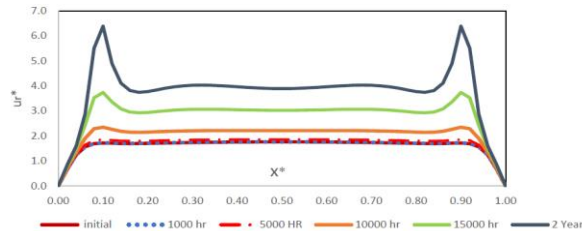


Fig.7
Distribution of radial displacement along the dimensionless axial direction after two years of creeping.

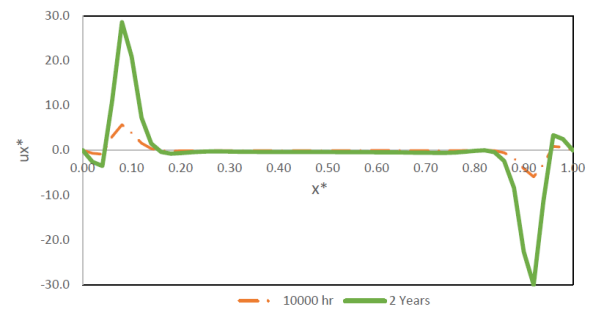
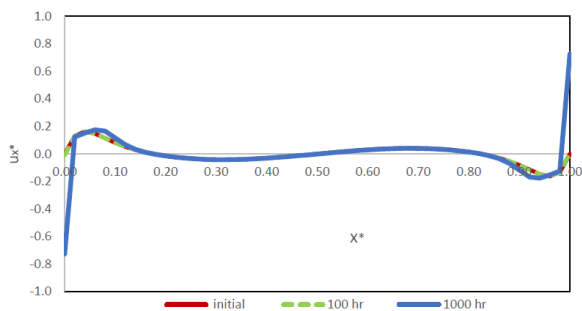


Fig.8
a) Distribution of axial displacement along the dimensionless axial direction after 1000 hours of creeping. b) Distribution of axial displacement along the dimensionless axial direction after two years of creeping.

Figs. 9, 10 indicate the effect of internal and the external pressure and heat flux on circumferential stress distribution in middle layer. When the load share of internal pressure is more than external pressure, positive circumferential stress is created in the structure. By reducing this share, the amount of circumferential stress created in the body is reduced, and even compressive circumferential stress may be created in the structure. Fig. 10 shows as

heat transfer from the outside surface increases, and the temperature becomes limited. Therefore, the circumferential stress is reduced. Fig. 11 show the history of effective creep rates over time and increases over time.

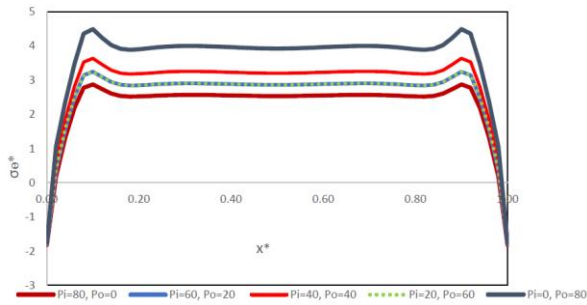


Fig.9
Effect on internal and external pressure on normalized circumferential stress distribution in the middle layer after one-year creeping.

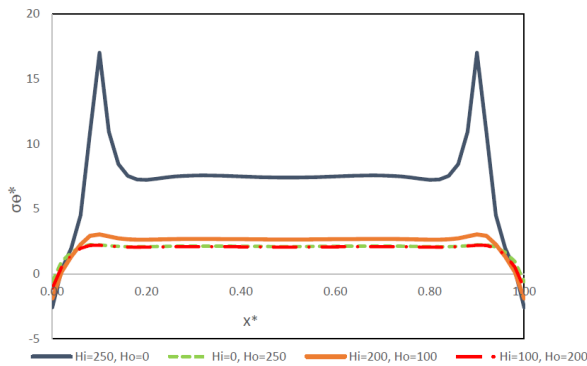


Fig.10
Effect of internal and external heat flux on circumferential stress distribution in the middle layer after one-year creeping.

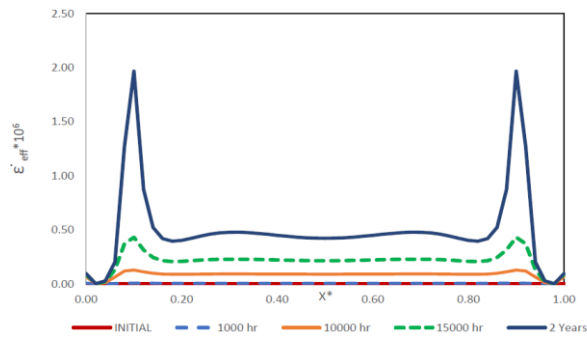


Fig.11
History of effective creep rate in the middle layer of the cylinder over time.

Figs. 12-15 indicate circumferential stress, shear stress and radial displacement respectively in different layers after 1,000 hours. The maximum and minimum circumferential stress occurs in the inner layer and outer layer respectively. Radial displacements in different layers are not much different. The inner layer also sees the most effective stress.

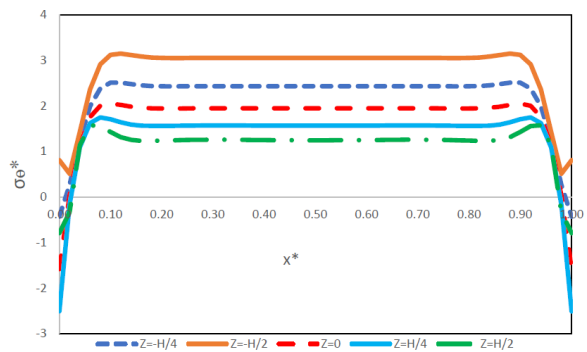


Fig.12
Circumferential stress after 1,000 hours in different layers.

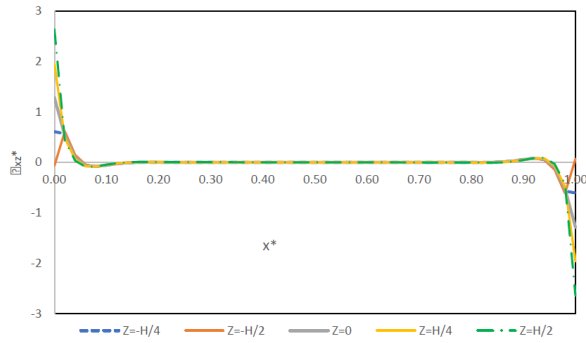


Fig.13
Shear stress after 1,000 hours in different layers.

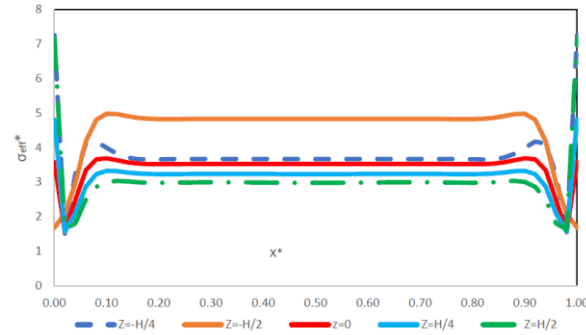


Fig.14
Effective stress after 1,000 hours in different layers.

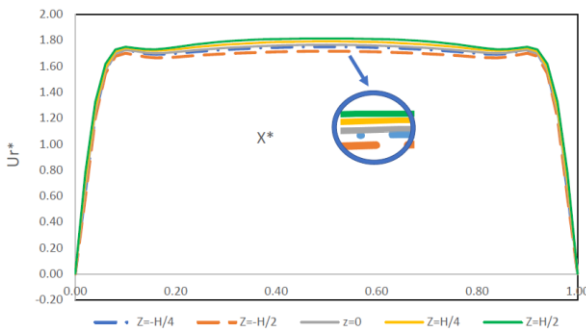


Fig.15
Radial displacement after 1,000 hours in different layers.

To validate the results, the cylinder is considered in the absence of a temperature field. In the middle of the cylinder ($x=L/2$) and the middle layer ($z=0$) the linear elasticity theory in plain strain condition and the first-order shear deformation theory are comparable. However, the problem is modeled in ABAQUS and the thermoelastic and creep analysis were done. The two theories and the FEM solution compare together for thermoelastic solution and creep analysis. According to Table 1, the circumferential stresses in the initial time for both theories are close together, 0.53% deviation from the FSDT theory for the PET theory and 0.59% from PET theory for FEM solution. However, the deviation between the two theories due to accumulation in the creep phenomenon increased to 8.72% after 1,000 hours and 2.39% PET compared to FEM.

The radial displacement in initial time deviation is 0.23%, but after 1,000 hours, it reached 8.13% and in the same way deviation from PET for FEM are 0.72% and 7.2% for initial time and 1000 hours.

Table 1
The numerical result of different solutions.

$X=L/2, z=0$	Theory	Initial	100 hour	1000 hour
U_r	PET	0.03875 mm	0.03782 mm	0.03602 mm
	FSDT	0.03786 mm	0.03778 mm	0.0392 mm
	FEM	0.03812 mm	0.03813 mm	0.0386 mm
σ_θ	PET	156.16 Mpa	156.04 Mpa	147.66 Mpa
	FSDT	155.32 Mpa	155.4 Mpa	161.76 Mpa
	FEM	157.09 Mpa	157.12 Mpa	157.89 Mpa

The PET theory cannot be used in two dimensional temperature solution, so in order to show the effectiveness and accuracy of FSDTT theory, a comparison between responses of the present theory and FEM can be made. Table 2 show a good agreement between two theories. In another part of this research, the effect of temperature increase on the creep phenomenon has been investigated.

Table 2

The numerical result of different solutions in the presence of temperature.

$X=L/2, z=0$	Theory	Initial	100 hour	1000 hour
U_r	FSDT	0.07044 mm	0.07045 mm	0.07061 mm
	FEM	0.07047 mm	0.07143 mm	0.07156 mm
σ_θ	FSDT	155.31 Mpa	155.32 Mpa	155.75 Mpa
	FEM	157.12 Mpa	158.53 Mpa	158.89 Mpa

The time required for each temperature to reach a displacement of 0.2 mm at the middle point of the cylinder is obtained Table3.

Table 3

The effect of temperature increase on the creep phenomenon.

The temperature of the two ends	Time passed	Percentage of reduction in time
100°C	5880 hr
200°C	5130 hr	12%
300°C	4430 hr	15.8%

In the middle layer of the cylinder, the radial displacement is examined as the temperature increases. According to the Table 4, the percentage of changes from the previous case was reported.

Table 4

The effect of temperature on radial displacement.

The temperature of the two ends	U_r at middle point	Percentage of increase
50°C	0.077 mm	----
100°C	0.22 mm	185%
200°C	0.256 mm	16.3%
300°C	0.313 mm	22.2%

If the temperature of the two ends of the cylinder is doubled, the time to reach the radial displacement of 0.2 mm at the center point of the cylinder is reduced by 12.6%, and if this temperature is tripled, it requires 24.6% less time that the central point of the cylinder reaches the displacement of 0.2 mm. Table 5 shows that the multiplying of temperature in two ends of cylinder will dramatically increase the rate of middle point radial displacement. Therefore, with temperature control, the creep behavior can be controlled, and by increasing the temperature, the emergence of creep phenomena occurs rapidly.

Table 5

The effect of increasing temperature in the middle point on radial displacement.

The temperature of the two ends	Time passed	Radial displacement of middle point
100°C	7000 hr	0.24 mm
200°C	7000 hr	0.3 mm
300°C	6370 hr	0.32 mm
400°C	75 hr	0.9 mm

7 CONCLUSIONS

This paper presents a semi-analytical solution for obtaining an axisymmetric cylinder that is subjected to internal pressure and internal and external heat flux with clamped-clamped boundary conditions. A thermoelastic, analysis of the problem was made using the energy method, first-order shear deformation theory, and first-order temperature. Assuming the Baily-Norton model, the creep behavior was used for stimulation. Using the numerical method, the history of stresses and displacement was discussed. Creep analysis using the FSDTT theory is the innovation presented by this research. In general, the extracted conclusions are as follows:

- a) Over time, the amount of stress and displacement increases, and in some cases, it is more significant.
- b) The pressure and heat flux have direct effect on the creep behavior. The more the internal pressure, the more the circumferential stress, and despite the internal heat flux, the more the circumferential stress will be.
- c) As shown, the temperature has an exponential effect on creep behavior. Thus, at high temperatures, the life of the structure is significantly reduced.
- d) The inner layer has always been under the highest stress.

ACKNOWLEDGMENTS

Support of Dr. Mohammad Parhizkar Yaghoobi in completing this research work is acknowledged with thanks.

REFERENCES

- [1] Loghman A., Shokouhi N., 2009, Creep damage evaluation of thick-walled spheres using a long-term creep constitutive model, *Journal of Mechanical Science and Technology* **23**(10): 2577-2582.
- [2] Chen J.J., Tu S.T., Xuan F.Z., Wang Z.D., 2007, Creep analysis for a functionally graded cylinder subjected to internal and external pressure, *The Journal of Strain Analysis for Engineering Design* **42**(2): 69-77.
- [3] Samaisim G.F., Bidgoli M., 2022, Review of thermoelastic thermal properties and creep analysis of functionally graded cylindrical shell, *Australian Journal of Mechanical Engineering*, doi:10.1080/14484846.2022.2100045.
- [4] Jahed H., Bidabadi J., 2003, An axisymmetric method of creep analysis for primary and secondary creep, *International Journal of Pressure Vessels and Piping* **80**(9): 597-606.
- [5] Mangel S.K., Kapoor N., Singh T., 2013, Steady-state creep analysis of functionally graded rotating cylinder, *Strain* **49**(6): 457-466.
- [6] Jones N., Sullivan P. F., 1976, On the creep buckling of a long cylindrical shell, *International Journal of Mechanical Science* **18**(5): 209-213.
- [7] Stowell E.Z., Gregory R. K., 1965, Steady-state biaxial creep, *Journal of Applied Mechanics* **32**: 37-42.
- [8] King R.H., Mackie W., 1967, Creep of thick-walled cylinders, *Journal of Basic Engineering* **89**: 877-884.
- [9] Gupta S. K., Dharamani R. L., Rana V. D., 1979, Creep transition in torsion, *International Journal Non-linear Mechanics* **13**(5): 303-309.
- [10] Murakami S., Iwatsuki S., 1970, Steady state creep of circular cylindrical shells, *Bulletin of JSME* **14**(73): 615-623.
- [11] Bhatnagar N.S., Kulkarni P.S., Arya V.K., 1984, Creep analysis of an internally pressurized orthotropic rotating cylinder, *Nuclear Engineering and Design* **83**(3): 379-388.
- [12] Loghman A., Wahab M.A., 1996, Creep damage simulation of thick-walled tubes using the projection concept, *International Journal of Pressure Vessels and Piping* **67**(1): 105-111.
- [13] You L.H., Ou H., Zheng Z.Y., 2007, Creep deformation and stresses in thick-walled cylindrical vessels of functionally graded material subjected to internal pressure, *Composite Structure* **78**(2): 285-291.
- [14] Altenbach H., Gorash Y., Naumenko K., 2008, Steady-state creep of a pressurized thick cylinder in both the linear and the power law ranges, *Acta Mechanica* **195**: 263-274.
- [15] Loghman A., Atabakhshian V., 2012, Semi-analytical solution for time-dependent creep analysis of rotating cylinder made of anisotropic exponentially graded material (EGM), *Journal of Solid Mechanics* **14**: 313-326.
- [16] Thakur P., 2013, Creep transition stresses of orthotropic thick-walled cylinder under combined axial load under internal pressure, *Facta Universitatis Series Mechanical Engineering* **11**(1): 13-18.
- [17] Moradi M., Loghman A., 2018, Non-axisymmetric time-dependent creep analysis in a thick-walled cylinder due to the thermo-mechanical loading, *Journal of Solid Mechanics* **10**(4): 845-863.
- [18] Loghman A., Askari Kashan A., Younesi Bidgoli M., Shajari A.R., Ghorbanpour Arani A., 2013, Effect of particle content, size and temperature on magneto-thermo-mechanical creep behavior of composite cylinders, *Journal of Mechanical Science and Technology* **27**(4): 1041-1051.
- [19] Ahmad J., Wahab M. A., 2015, Thermoelastic and creep analysis of a functionally graded rotating cylindrical vessel with internal heat generation, *World Journal of Engineering* **12**: 517-532.
- [20] Thakur P., Gupta N., Singh S. B., 2017, Creep strain rates analysis in cylinder under temperature gradient materials by using Seth's theory, *Engineering Computations* **34**(3): 1020-1030.
- [21] Kashkoli M.D., Tahan Kh. N., 2017, Time dependent thermomechanical creep behavior of FGM thick hollow cylindrical shells under non-uniform internal pressure, *International Journal of Applied Mechanics* **9**: 1750086-1750112.
- [22] Kashkoli M. D., Tahan Kh. N., Zamani-Nejad M., 2018, Thermo-Mechanical creep analysis of FGM thick cylindrical pressure vessels with variable thickness, *International Journal of Applied Mechanics* **10**(1): 1850008-1850045.
- [23] Kashkoli M.D., Tahan Kh N., 2017, Time dependent creep analysis for life assessment of cylindrical vessels using first order shear deformation theory, *Journal of Mechanics* **33**(4): 461-474.

- [24] Ghannad M., Parkizkar Yaghoobi M., 2015, A thermoelectricity solution for thick cylinders subjected to thermomechanical loads under various boundary condition, *International Journal of Advanced Design and Manufacture Technology* **8**(4): 1-13.
- [25] Ghannad M., Parkizkar Yaghoobi M., 2016, 2D thermo elastic behavior of a FG cylinder under thermomechanical loads using a first order temperature theory, *International Journal of Pressure Vessels and Piping* **149**: 75-92.
- [26] Tzou H. S., Bao Y., 1995, A theory on anisotropic piezothermoelastic shell laminates with sensor/actuator applications, *Journal of Sound and Vibration* **184**(3): 453-473.
- [27] Yang Y.Y., 2000, Time-dependent stress analysis in functionally graded materials, *International Journal of Solids and Structures* **37**(51): 7593-7608.